Monte Carlo calculations of phase diagrams for a fluid confined in a disordered porous material

K. S. Page and P. A. Monson
Department of Chemical Engineering, University of Massachusetts, Amherst, Massachusetts 01003
(Received 10 June 1996)

A Monte Carlo simulation study of the phase diagram of an off-lattice molecular model of a fluid in a disordered porous material is presented. The molecular model consists of a Lennard-Jones 12-6 fluid confined in a rigid matrix of spheres with size parameters representative of methane in a silica xerogel. The matrix spheres are arranged in a configuration from an equilibrium hard-sphere system, although in some cases a fcc arrangement was considered in order to study the effect of translational order in the matrix. Various strengths of attraction between the fluid molecules and matrix particles have been considered, including the case of complete repulsion. The fluid-phase diagram shows effects of confinement, wetting, and matrix disorder. The results of this study provide evidence for two fluid-phase transitions. One transition is analogous to the bulk vapor-liquid transition, while the second is related to the wetting properties of the fluid in the more confined regions of the matrix. A key feature of our results is the inhomogeneity and disorder of the equilibrium phases in the system. [S1063-651X(96)05312-3]

PACS number(s): 05.70.Fh, 64.70.Fx, 68.45.Gd

I. INTRODUCTION

The phase behavior of fluids and fluid mixtures in disordered porous materials has been the subject of much recent interest from both an experimental and a theoretical point of view [1], reflecting both its significant practical importance and the interesting conceptual challenges it offers. The observed behavior can be determined by a variety of effects including confinement, wetting phenomena, and how these are affected by the disordered microstructure. Experimental studies of vapor-liquid and liquid-liquid phase separation have been made in a variety of porous glasses and gels [2]. These studies have shown that the phase diagram, as well as the dynamics of phase separation, is dramatically altered by the presence of the gel. Even extremely dilute porous materials such as aerogels can have profound effects on fluid behavior, as illustrated by the case of ^{4}He in an aerogel [3], which exhibits an extremely narrow vapor-liquid coexistence curve. Although work in this area has progressed for more than a decade, a complete understanding of the experimental phenomena has not yet been achieved.

Among the theoretical approaches that have been used in understanding these systems the most popular has been the random field Ising model [4] (RFIM). The random field describes the spatially varying preference of the disordered medium for the different fluid phases. There is no effect of confinement in the model and correlations between the random fields that would model correlation effects of potential importance in real systems are usually neglected. In addition, the model does not provide a description of the role of wetting. Nevertheless, the central idea of inhomogeneous and disordered equilibrium phases that underlies the RFIM is a key concept in understanding these kinds of systems. From a somewhat different perspective, Liu and co-workers [5] have suggested that the phase-separation dynamics for these systems may be determined by the geometry of the wetting phases that can be modeled within a single-pore approach. Another line of attack has been application of methods of from liquid-state statistical mechanics to off-lattice molecular models of fluids in porous materials [6] and this approach has recently been applied to the study of phase equilibrium [7,8].

The purpose of the present paper is to present a detailed account of a Monte Carlo simulation study [9] of the phase diagram of an off-lattice molecular model of a fluid confined in a disordered material. The model provides a reasonably realistic picture of the microstructure of a disordered porous material, in this case a silica xerogel, while remaining computationally tractable. It includes effects of confinement, wetting, and matrix disorder on the fluid thermodynamics in realistic way. The phase behavior determined in this work shows several interesting effects. The critical temperature for the vapor-liquid transition is lower than in the bulk, as would be expected for a confined system [10]. The vapor-liquid coexistence curve is much narrower than that in the bulk and this appears to be a consequence of both the wetting behavior of the fluid in the matrix and the disorder in the matrix. The location of critical density relative to the bulk value is determined by the strength of the interaction between the fluid molecules and the porous matrix. In addition to a vapor-liquid transition, analogous to capillary condensation, our results provide evidence for a second transition that is associated with the wetting behavior of the fluid in the more dense regions of the matrix. A second transition with an apparently similar origin was recently predicted using a lattice model of a fluid in a porous material using the replica Ornstein-Zernike equation in the mean-spherical approximation [11]. A comparison with results for a translationally ordered matrix as well as computer graphics visualizations of the phases present reveal an important contribution to the behavior from the matrix disorder.

In Sec. II we describe the molecular model as well as the computer simulation techniques used in this work. We also discuss briefly the thermodynamics used in our phase equilibrium calculations. Section III presents our detailed results including adsorption isotherms, phase diagrams, and some computer graphics visualizations of the equilibrium phases in

the system. A summary of our results and conclusions is given in Sec. IV.

II. MOLECULAR MODEL AND MONTE CARLO SIMULATIONS

The molecular model used in this work is based on one used by Kaminsky and Monson [12] in studies of adsorption of simple molecules in silica xerogel. The adsorbent matrix is modeled via a configuration of hard spheres taken from an equilibrium hard-sphere Monte Carlo simulation. In this model the size ratio between the matrix spheres and fluid molecules is 7.055:1 and the volume fraction η of the hard-sphere system used to generate the matrix configuration is 0.386. The interaction between the fluid molecules and the matrix particles has been modeled in two ways. In one case the interaction was a purely repulsive hard-sphere interaction. In other cases attractive forces between the matrix particles and fluid molecules were described by the composite sphere potential in which each matrix sphere is treated as a continuum of interaction centers [12]. The potential provides a level of approximation similar to that given by the 9-3 potential [13] used for modeling interactions with plane surfaces and reduces to the 9-3 potential in the limit where the matrix to fluid particle size ratio becomes very large. If each matrix particle is modeled as a continuum of Lennard-Jones 12-6 interaction centers, the potential energy between a matrix particle and a fluid molecule is given by

$$u^{cs}(d)=\frac{16\pi\epsilon_{gs}\rho_s R^3}{3}\left[\frac{(d^6+\frac{21}{5}d^4R^2+3d^2R^4+\frac{1}{3}R^6)\sigma_{gs}^{12}}{(d^2-R^2)^9}-\frac{\sigma_{gs}^6}{(d^2-R^2)^3}\right], \tag{1}$$

where d is the distance from the center of the fluid molecule to the center of the matrix particle, ρ_s is the density of interaction sites in the matrix particles, R is the matrix particle radius, and σ_{gs} and ϵ_{gs} are the collision diameter and well depth for the 12-6 potential between the fluid molecule and a matrix particle interaction center. We use the values $\sigma_{gs}=0.8646\sigma_{gg}$ and $\epsilon_{gs}=2.287\epsilon_{gg}$, where the subscript gg denotes the fluid-fluid interaction parameters. In addition, we have $R=3.5275\sigma_{gg}$ and $\rho_s\sigma_{gg}^3=2.447$. These are the values used by Kaminsky and Monson [12]. This potential can be regarded as an approximation to a more detailed intermolecular potential developed by MacElroy and Raghavan [14] that incorporates the atomic structure of the silica particles making up the matrix. For the interactions between the fluid molecules a Lennard-Jones 12-6 potential truncated at 2.5 collision diameters was used.

In order to vary the strength of the attractive forces while maintaining an approximately constant porosity for the matrix we proceeded as follows. The composite sphere potential for methane in silica gel was divided into attractive and repulsive parts in the manner used in the Weeks-Chandler-Andersen perturbation theory [15]. Systems with the similar porosity but different attractive interaction strengths were then obtained by progressive addition of the attractive part of the potential to the repulsive reference potential. The resulting potential can be expressed as

$$\frac{u_{gs}(d)}{\epsilon_{gg}}=\begin{cases}u_{cs}(d)+(\alpha-1)u_{cs}(d_{\min}), & d<d_{\min}\\ \alpha u_{cs}(d), & d_{\min}\leq d\leq d_c\\ 0, & d>d_c.\end{cases} \tag{2}$$

In this last equation $\alpha=\epsilon_{gs}/\epsilon_{gs}^{(0)}$, where $\epsilon_{gs}^{(0)}$ is the well depth in the composite sphere potential used for methane in silica gel, d_c is the truncation in the adsorbent-adsorbate potential-energy calculation, and $d_{\min}$ is the value of d for which $u_{cs}(d)$ is a minimum. In this work we chose $d_c=7.055\sigma_{gg}$. Varying the strength of the fluid-matrix attractive forces has allowed us to investigate the effects of wettability on the phase diagram. This procedure produces a fluid-matrix potential in which the repulsive part varies much less with the value of ϵ_{gs} than does the repulsive part of the original composite sphere potential.

The Monte Carlo simulations used in this work were carried out in the grand canonical ensemble by the usual method [16]. Thirty-two matrix particles were used in a cubic cell with periodic boundaries. This leads to a simulation cell with dimensions of about $25\times25\times25$ fluid particle diameters. The number of fluid molecules in the system ranged from just a few at the lowest activities up to about 10^4 at the highest activities considered. The simulation runs typically involved (50×10^6)–(100×10^6) configurations for equilibration of the system from a given initial condition and an equal number for obtaining the ensemble averages. A configuration consisted of an attempted translation of a randomly chosen fluid molecule followed by either an attempted addition or removal of a fluid molecule. Cell lists were used to reduce the computer time taken to sum the interactions in the system. Most of our results are for a single configuration of the matrix since this was dictated by computational limitations. This might at first seem questionable since a 32-particle configuration may not be sufficiently representative of the statistical geometry of a hard-sphere system. However, in some cases we carried out calculations for other matrix configurations and the results were quite similar, as will be shown shortly.

In these systems the conditions for equilibrium between two phases at fixed temperature are the equalities of the chemical potentials and grand potential densities in the two phases. To determine the grand potential densities we have used thermodynamic integration methods. The grand potential density can be determined from a Monte Carlo simulation isotherm of fluid density versus chemical potential by integration of the Gibbs adsorption isotherm, i.e.,

$$d\phi=-\rho d\mu, \tag{3}$$

where $\phi=\Omega/V$ is the grand potential density, μ is the chemical potential, and ρ is the fluid density. For low-density states up to any phase transition this integration can be performed by starting in the Henry law limit where the fluid behaves as an ideal gas in an external field. For the dense phase it is necessary to determine the grand potential density at some reference state and then integrate the Gibbs adsorption isotherm starting from that state. To determine this reference state value we first determined an isotherm of the grand potential density at a temperature above the bulk critical temperature. The grand potential at lower temperatures for dense

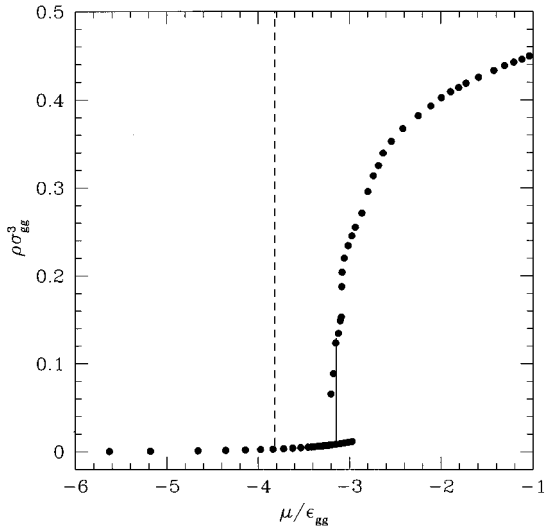

FIG. 1. Adsorption isotherm at the temperature $kT/\epsilon_{gg}=0.75$ for the 12-6 fluid in a hard-sphere matrix. The solid line is our estimate of the vapor-liquid tie line and the dashed line marks the saturation chemical potential for the bulk 12-6 fluid.

states could then determined by integration over temperature of the grand canonical Gibbs-Helmholtz equation

$$\left(\frac{\partial(\phi/T)}{\partial T}\right)_z = -\frac{\rho U_c}{T^2}, \tag{4}$$

where T is the temperature, U_c is the configurational energy per molecule, and z is the configurational activity or fugacity (which is equal to $e^{\mu_c/kT}$, where μ_c is the configurational chemical potential). In the cases at lower temperatures where, as we shall see, there are apparently two phase transitions on an isotherm, we have not used this procedure for the secondary transition but have simply used the step in the adsorption isotherms to estimate the location of the transitions.

III. RESULTS

We begin by considering the case of a completely repulsive hard-sphere interaction between the matrix and the fluid. Figure 1 shows an adsorption isotherm for a temperature well below the bulk critical temperature. This isotherm exhibits hysteresis between adsorption and desorption with a transition between fluid states of low and medium density. We have interpreted this transition as the analog of the vapor-liquid transition in the bulk. The value of the chemical potential at bulk saturation is marked on the graph and we see that the transition in the pore occurs at a higher chemical potential than that in the bulk, as should be expected for a system with repulsive fluid-matrix interactions [10,17]. A perhaps striking feature of this isotherm is the rather low value of the condensed phase density. We will return to this point shortly. First, however, we show some further results at the same temperature for three other realizations of the matrix. These adsorption isotherms are shown together with the first one in Fig. 2. We also compare the coexistence tie line obtained from an isotherm averaged over four matrix realizations with that shown in Fig. 1. This is shown in Fig. 3.

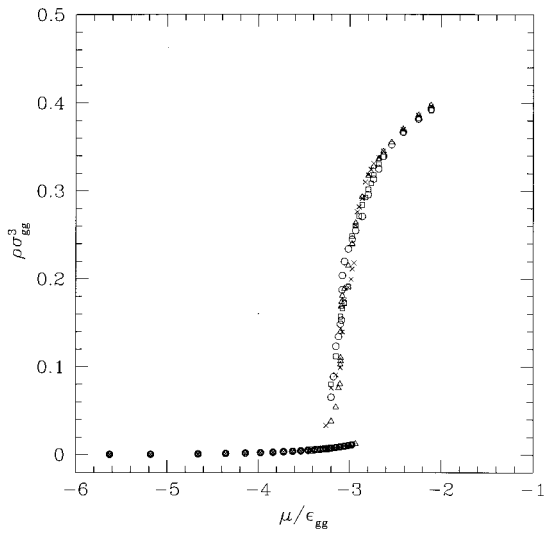

FIG. 2. Adsorption isotherms at the temperature $kT/\epsilon_{gg}=0.75$ for the 12-6 fluid in four different configurations of the hard-sphere matrix.

These comparisons show that, although we can expect some quantitative differences by averaging over larger numbers of matrix realizations, the qualitative picture should not change significantly.

In Figs. 2 and 3 of Ref. [9] we presented computer graphics visualizations of configurations from the Monte Carlo simulations for liquid and vapor states close to coexistence at one temperature. In both cases the spatial distribution of the molecules was seen to be highly inhomogeneous and disordered. This is the kind of picture that would be anticipated on the basis of the random field Ising model. What is particularly striking is that for the liquid phase there are extensive regions of the matrix that have very low fluid density.

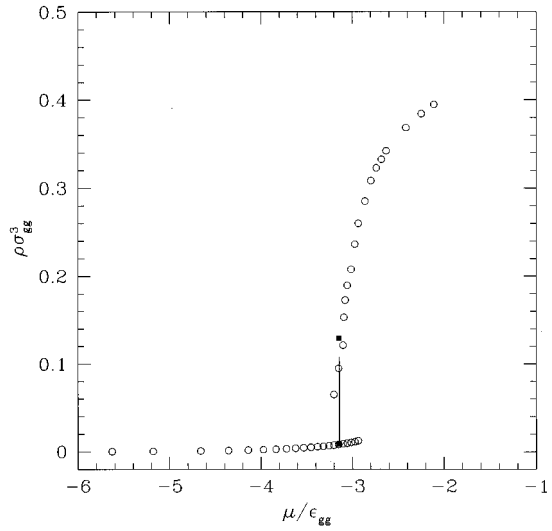

FIG. 3. Adsorption isotherm at the temperature $kT/\epsilon_{gg}=0.75$ for a 12-6 fluid in a hard-sphere matrix. The points are averages over the results in Fig. 2, the solid line is the calculated vapor-liquid equilibrium phase transition for the averaged isotherm, and the solid squares are the saturated vapor and liquid densities calculated for the isotherm in Fig. 1.

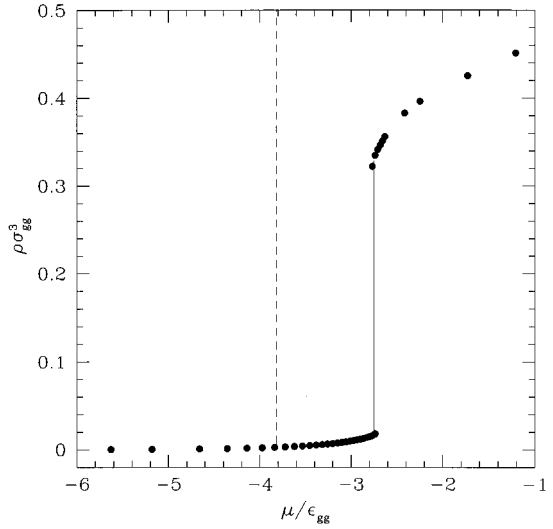

FIG. 4. Adsorption isotherm at the temperature $kT/\epsilon_{gg}=0.75$ for a 12-6 fluid in a fcc hard-sphere matrix. The solid line is the calculated vapor-liquid equilibrium phase transition and the dashed line marks the saturation chemical potential for the bulk 12-6 fluid.

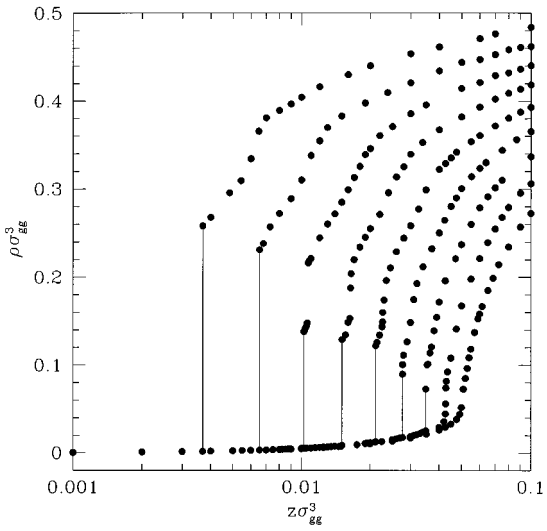

FIG. 6. Adsorption isotherms for the 12-6 fluid in a hard-sphere matrix. The isotherms from left to right correspond, respectively, to the temperatures $kT/\epsilon_{gg}=0.6$, 0.65, 0.7, 0.75, 0.8, 0.85, 0.9, 0.95, and 1.0. The solid lines are calculated tie lines for the vapor-liquid transitions.

These are the regions where the matrix density is highest and where the repulsive fluid-matrix interaction favors low fluid density.

To investigate further the role of the disorder we have for one of the temperatures studied a system in which the matrix spheres are arranged in a fcc structure. At the same temperature this system exhibits a much larger density change during the vapor-liquid transition than for the disordered system, as shown in Fig. 4. Moreover, density distributions of the fluid for both liquid and vapor phases in this system are periodic. This can be seen in Fig. 5, where we show a configuration of this system from a state close to the saturated liquid.

We have studied adsorption isotherms at several other temperatures for the disordered matrix and this has allowed us to construct the phase diagram for the fluid. The adsorption isotherms are shown as a ρ vs μ plot in Fig. 6 with the corresponding ϕ vs ρ plot in Fig. 7. The T vs ρ phase coexistence plot is shown in Fig. 8. In this figure the bulk vapor-liquid coexistence curve is also shown as calculated from the accurate equation of state of Johnson, Zollweg, and Gubbins [18], corrected for the effect of truncating the potential. The results, as well as those in Figs. 6 and 7, indicate the presence of two transitions between fluid phases in the system. We associate the larger coexistence region with the vapor-liquid transition. Evidently, the vapor-liquid coexistence re-

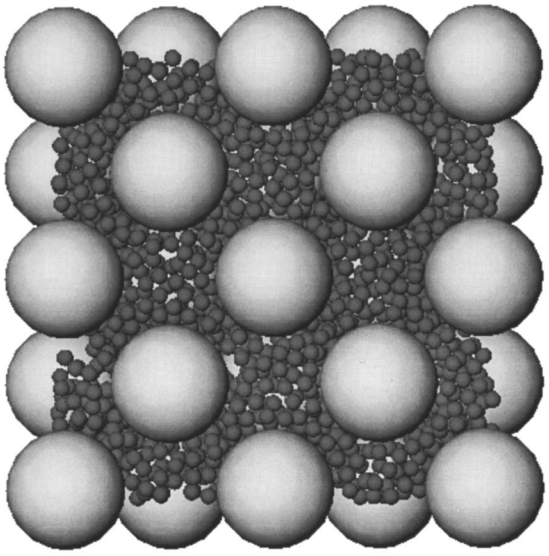

FIG. 5. Computer graphics visualization of a configuration of the 12-6 fluid in a fcc hard-sphere matrix near the saturated liquid state at a temperature $kT/\epsilon_{gg}=0.75$.

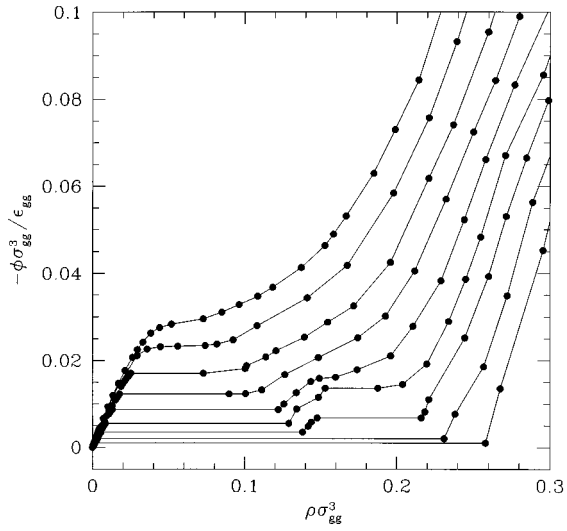

FIG. 7. Grand potential density isotherms calculated via thermodynamic integration for the 12-6 fluid in a hard-sphere matrix. The isotherms from left to right correspond, respectively, to the temperatures $kT/\epsilon_{gg}=0.6$, 0.65, 0.7, 0.75, 0.8, 0.85, 0.9, 0.95, and 1.0. The points are our calculated values and the lines are drawn as a guide to the eye.

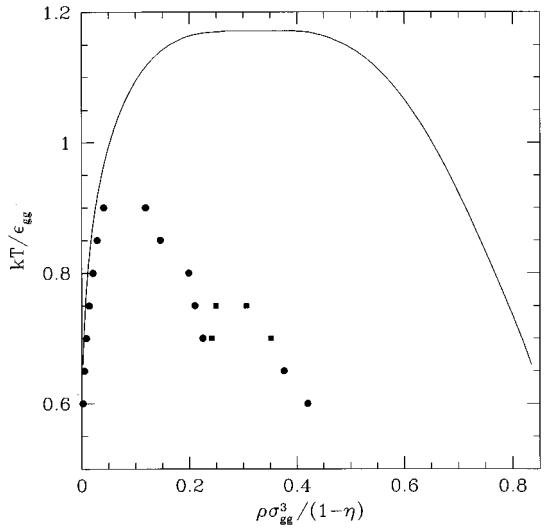

FIG. 8. Phase diagram for a Lennard-Jones 12-6 fluid in a hard-sphere matrix. The solid circles are the saturated vapor and liquid densities and the solid squares represent the coexistence densities at the second transition. The solid line is the coexistence curve for the bulk fluid.

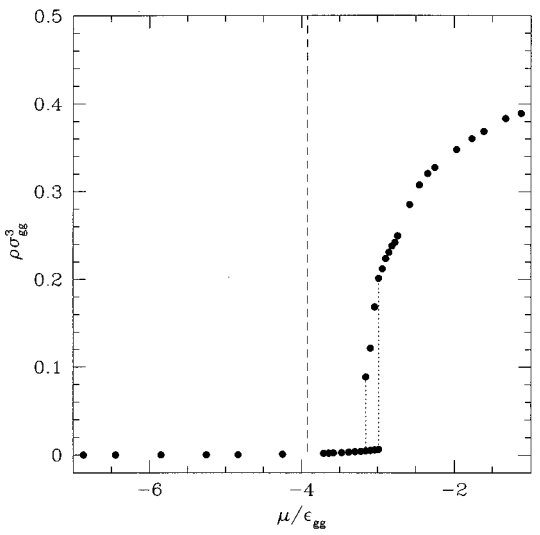

FIG. 9. Adsorption isotherm at the temperature $kT/\epsilon_{gg}=0.7$ and $\alpha=0.0$ for the 12-6 fluid in a composite sphere matrix. The dotted lines mark the limits of the hysteresis behavior and the dashed line marks the saturation chemical potential for the bulk 12-6 fluid.

gion appears at lower temperatures than for the bulk, as would be expected for such a confined system. Also the condensed phase densities are lower than those in the bulk and the coexistence curve is substantially narrower. The shift in the coexistence curve and its narrowness are to a significant extent associated with the repulsive interaction between the fluid and the matrix, which promotes a low fluid density in the neighborhood of the matrix particles and acts to lower the density of condensed phases in the system. But, as we have already seen, the matrix disorder also plays a role. Some care should be taken in making comparisons of coexistence densities between the bulk and confined fluids for systems like the present one since the volume fraction of the solid in matrix needs to be accounted for and the finite size of the fluid molecules prevents the void space from being uniformally accessible. Nevertheless, in view of the magnitude of the effects seen here it is reasonable to divide the fluid density by the void fraction 1-η of the hard-sphere matrix (the void fraction is understood to be unity for the bulk case) to make an approximate comparison with the bulk coexistence curve as is done in Fig. 8.

We turn now to the second coexistence region that occurs at low temperature on the high-density side of the vapor-liquid coexistence region. This transition is associated with the change in the fluid density in the high-density regions of the matrix. The physics involves a competition between the repulsive fluid-matrix interactions, which favor a lower fluid density in the confined regions of the matrix, and the attractive forces between the fluid molecules, which tend to stabilize a high-density phase (where high density permeates a much wider region of the matrix than seen in Fig. 2 of Ref. [9]). The analogy with a predrying transition for a liquid in contact with a plane surface is a tempting one, although the drying transition is thought to be either second order or weakly first order [19], making the possibility of observing a predrying transition for a plane surface unlikely. Our estimates of the phase coexistence for the second transition are not as precise as for the high-temperature vapor-liquid transition since they are based only on steps observed in the adsorption isotherms. As a measure of the uncertainty we note that the isotherm in Fig. 1 shows a small step at high density and we have used this as our estimate of the coexistence points at $kT/\epsilon_{gg}=0.75$ in Fig. 8. The uncertainty in the estimate at this temperature is exacerbated by its proximity to the critical temperature of the second transition and the sensitivity of the results to the matrix configuration. On the other hand, we did check that the second transition was clearly visible for a second matrix configuration at $kT/\epsilon_{gg}=0.7$.

Next we consider the case of attractive fluid-matrix interactions. We have studied various strengths of the fluid-matrix attractive interaction strength at a single temperature and have calculated the phase coexistence and the entire fluid phase diagram for one value of α. Figures 9–12 show adsorption isotherms for four increasing values of α starting with $\alpha=0$. The isotherm for $\alpha=0$ in Fig. 9, where there is only a soft repulsive matrix-fluid interaction, is very similar to that shown in Fig. 1 for the hard-sphere matrix-fluid interaction, as should be expected. Notice the changes in the isotherm in passing from $\alpha=0$ in Fig. 9 to $\alpha=0.25$ in Fig. 10, where we see that liquid phase has a much higher density. This is because the attractive fluid-matrix interactions allow the high-density fluid to permeate the dense regions of the matrix. There is slight evidence on this isotherm for the second transition in the high-density region that was seen for the hard-sphere matrix-fluid interaction at lower temperature. As we increase the strength of the attractive interaction still further to $\alpha=0.375$ (Fig. 11) we see that the density of the liquid phase is increased further and now there is new behavior on the low-density branch of the isotherm with a second phase transition from low density to moderate density in the vapor phase. This transition is again associated with the wetting behavior of the fluid in the more dense regions of the matrix and again involves high-density fluid permeating the more confined regions of the matrix. There is some resem-

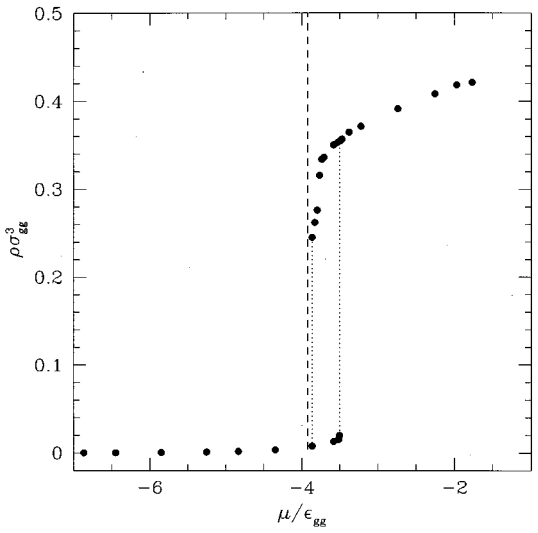

FIG. 10. Adsorption isotherm at the temperature $kT/\epsilon_{gg}=0.7$ and $\alpha=0.25$ for the 12-6 fluid in a composite sphere matrix. The dotted lines mark the limits of the hysteresis behavior and the dashed line marks the saturation chemical potential for the bulk 12-6 fluid.

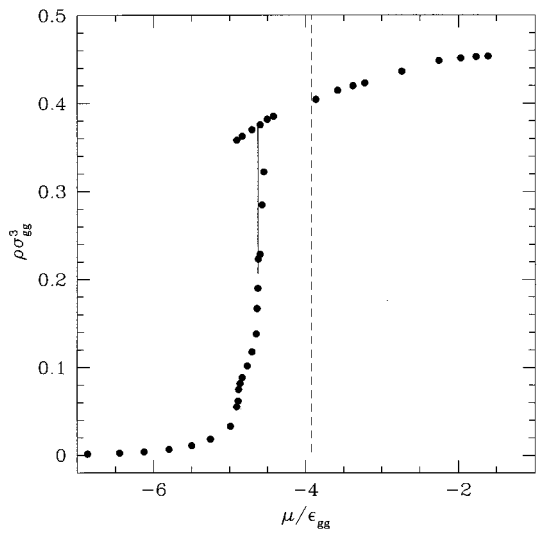

FIG. 12. Adsorption isotherm at the temperature $kT/\epsilon_{gg}=0.7$ and $\alpha=0.5$ for the 12-6 fluid in a composite sphere matrix. The solid line gives the calculated vapor-liquid equilibrium tie line and the dashed line marks the saturation chemical potential for the bulk 12-6 fluid.

blance between this transition and the prewetting transition for a plane surface and indeed the adsorption isotherms are quite similar to those seen for a planar fluid-solid system exhibiting prewetting [20].

By increasing the strength of the attractive matrix-fluid still further to $\alpha=0.5$ we obtain the isotherm shown in Fig. 12. We see that the second transition has disappeared except for a slight shoulder in the isotherm (as we shall see, the second transition appears at lower temperature for this system) and the vapor-liquid transition is narrowed and shifted to high density. We note that, as expected, the vapor-liquid transition region moves to a lower value of the chemical potential as we increase α at fixed temperature [10,17].

Figures 13 and 14 show snapshots from our Monte Carlo simulations for liquid and vapor states from the isotherm in Fig. 12, respectively, close to coexistence. We again see that the phases are inhomogeneous and disordered. In this case the matrix-fluid interaction acts to create a high-density disordered vapor state in contrast to the low-density disordered liquid state created by the repulsive matrix-fluid interaction as shown in Fig. 2 of Ref. [9].

Adsorption isotherms for a range of temperatures are shown in Fig. 15 for $\alpha=0.5$ and Fig. 16 shows the T vs ρ phase diagram we have determined. Once again we see evi-

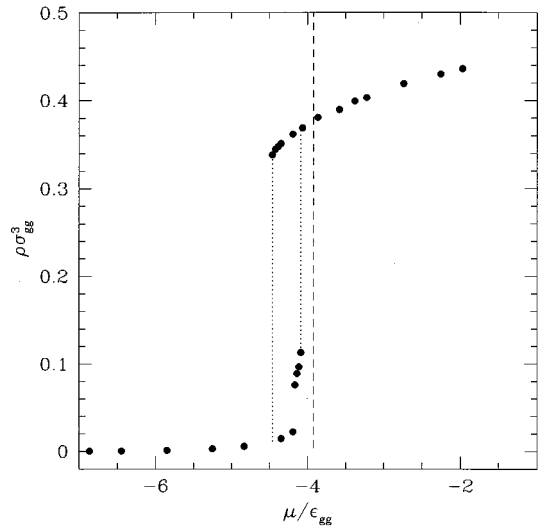

FIG. 11. Adsorption isotherm at the temperature $kT/\epsilon_{gg}=0.7$ and $\alpha=0.375$ for the 12-6 fluid in a composite sphere matrix. The dotted lines mark the limits of the hysteresis behavior and the dashed line marks the saturation chemical potential for the bulk 12-6 fluid.

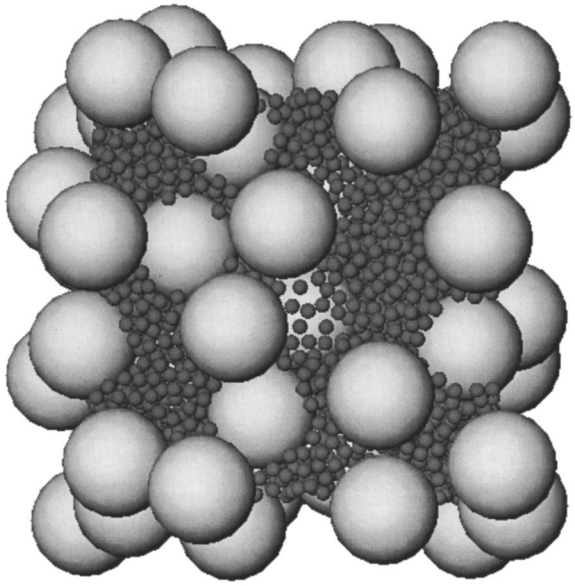

FIG. 13. Computer graphics visualization of a configuration of the fluid in the composite sphere matrix with $\alpha=0.5$ near the saturated liquid state at a temperature $kT/\epsilon_{gg}=0.7$.

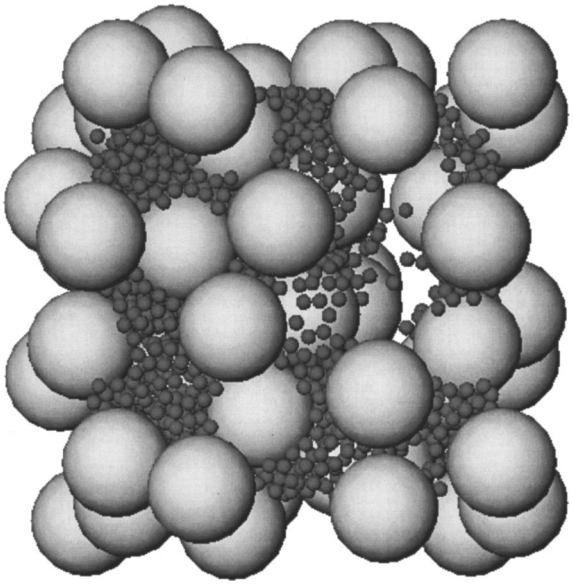

FIG. 14. Computer graphics visualization of a configuration of the fluid in the composite sphere matrix with $\alpha=0.5$ near the saturated vapor state at a temperature $kT/\epsilon_{gg}=0.7$.

dence for two phase transitions. As before we associate the larger coexistence region with the vapor-liquid transition. Consistent with the behavior seen in the adsorption isotherms, this coexistence region is now shifted to higher density than for the bulk and is quite narrow. The shift of the coexistence curve and its narrowness are again strongly associated with the attractive interaction between the fluid and the matrix, which promotes a high fluid density in the neighborhood of the matrix particles and increases the density of the vapor phase in the system. However, comparisons we have made with results for a fcc matrix again reveal a substantial role for the disorder. We again emphasize the significantly more uncertainty in our estimate of the second transition than for the vapor-liquid transition.

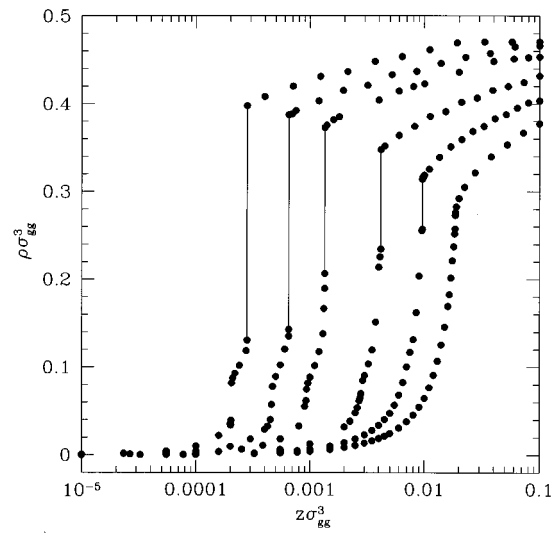

FIG. 15. Adsorption isotherms for 12-6 fluid in a composite sphere matrix with $\alpha=0.5$. The isotherms from left to right correspond, respectively, to the temperatures $kT/\epsilon_{gg}=0.6$, 0.65, 0.7, 0.8, 0.9, and 1.0. The solid lines are the calculated vapor-liquid equilibrium tie lines.

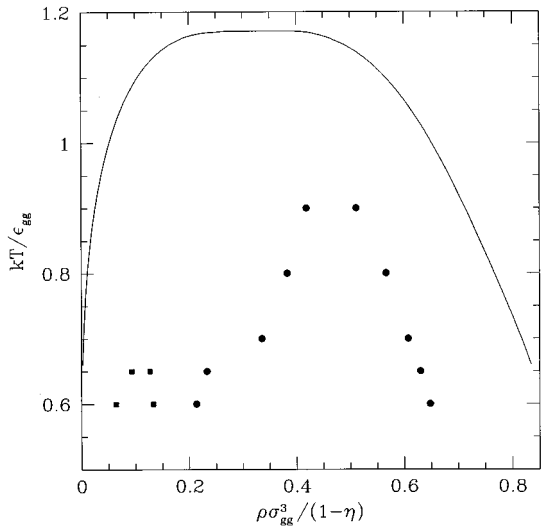

FIG. 16. Phase diagram for the 12-6 fluid in a composite sphere matrix with $\alpha=0.5$. The solid circles are the saturated vapor and liquid densities and the solid squares represent the coexistence densities at the second transition. The solid line is the coexistence curve for the bulk 12-6 fluid.

IV. SUMMARY AND CONCLUSIONS

We have presented results from a Monte Carlo simulation study of phase transitions in an off-lattice model of a fluid in a disordered porous material. The primary conclusions from this work can be summarized as follows: (i) the fluid phase diagram is substantially modified in the porous material; (ii) the critical temperature is lower than that in the bulk; (iii) the critical density and width of the vapor-liquid coexistence region depends upon the relative strength of fluid-solid and fluid-fluid attractive interactions, but is also influenced by the matrix disorder; (iv) the coexisting phases in the system exhibit a high degree of spatial inhomogeneity and disorder; and (v) there is evidence of an additional phase transition at lower temperature associated with wetting or drying behavior of the fluid in the more confined regions of the matrix.

Our results indicate that effects of confinement, wetting, and matrix disorder are all important in the system. A successful theoretical treatment must incorporate all these effects. We should note that the simple mean-field theory that has recently been presented [7] predicts only the suppression of the critical temperature and the lowering of the critical density. The effects of wetting or drying and the second phase transition are not predicted.

The picture of the coexisting phases in these systems as inhomogeneous and disordered fluid states is quite different from that associated with the traditional treatment of capillary condensation. The wetting or drying effects are coupled to the matrix disorder in a way that we do not believe can be accounted for based on a pore size distribution model.

Although the present study has involved a large number of Monte Carlo simulations for a quite large system (at least in terms of the number of fluid particles), our study is far from exhaustive. There remain several questions for future

work. Certainly it would be useful to investigate averages over larger numbers of matrix configurations to see how sensitive the phase diagram, especially with respect to the second transition, would be to such averaging, even though at this point we do not anticipate qualitative changes. Increasing the number of matrix particles would also be of interest, as well as varying the porosity and perhaps the connectivity of the matrix.

Our system is not directly comparable to any of the systems where phase transitions of fluids in disordered materials have been studied experimentally [2]. The closest experimental system to that studied here would be adsorption of methane in a silica xerogel [12]. However, the attractive matrix-fluid interactions we have used in our calculations are considerably weaker than for methane in silica xerogel. In fact, calculations we have done for a system more closely representative of methane in silica gel indicate that the attractive matrix-fluid interactions create a field sufficiently strong as to suppress all fluid phase transitions. Nevertheless, we believe there is a case to be made for further studies of fluids in xerogels at temperatures where phase transitions might occur. Indeed there are already experimental data for xenon in silica gel [21] that show the presence of hysteresis loops in the adsorption isotherms indicative of capillary condensation. These hysteresis loops are similar to those observed for xenon in porous glasses [22]. In the latter case the hysteresis loops have been analyzed [22] using density-functional theory for single pores together with models of the microstructure that treat the system either as a distribution of independent pores or as an interconnected network of pores. Studies of molecular models like the present one may also help clarify the hysteresis behavior in such systems.

Finally, the molecular models used here can also be studied using theories based on approximate closures to the replica Ornstein-Zernike equations [6,8,11]. It will be of considerable interest to use our results to test the theoretical predictions in the region of the phase transitions.

ACKNOWLEDGMENTS

The authors are grateful to E. Kierlik, J. Machta, M. L. Rosinberg, and G. Tarjus for helpful discussions and to the U.S. National Science Foundation for financial support (Grants Nos. CTS-9417649 and INT-9216943).

[1] For a review see B. J. Frisken, A. J. Liu, and D.S. Cannell, Mater. Res. Bull. **29**, 19 (1994).

[2] J. V. Maher, W. I. Goldburg, D. W. Pohl, and M. Lanz, Phys. Rev. Lett. **53**, 60 (1984); M. C. Goh, W. I. Goldburg, and C. M. Knobler, *ibid*. **58**, 1008 (1987); S. B. Dierker and P. Wilzius, *ibid*. **58**, 1865 (1987); S. B. Dierker, B. S. Dennis, and P. Wilzius, J. Chem. Phys. **92**, 1320 (1990); S. B. Dierker and P. Wilzius, Phys. Rev. Lett. **66**, 1185 (1991); B. J. Frisken, F. Ferri, and D. S. Cannell, *ibid*. **66**, 2754 (1991); B. J. Frisken and D. S. Cannell, *ibid*. **69**, 632 (1992); A. P. Y. Wong, S. B. Kim, W. I. Goldburg, and M. H. W. Chan, *ibid*. **70**, 954 (1993); B. J. Frisken, F. Ferri, and D. S. Cannell, Phys. Rev. E **51**, 5922 (1995).

[3] A. P. Y. Wong and M. H. W. Chan, Phys. Rev. Lett. **65**, 2567 (1990).

[4] F. Brochard and P. G. de Gennes, J. Phys. Lett. **44**, L785 (1983); P. G. de Gennes, J. Phys. Chem. **88**, 6469 (1984); A. Maritan, M. R. Swift, M. Cieplak, M. H. W. Chan, M. W. Cole, and J. R. Banavar, Phys. Rev. Lett. **67**, 1821 (1991).

[5] A. J. Liu, D. J. Durian, E. Herbolzheimer, and S. A. Safran, Phys. Rev. Lett. **65**, 1897 (1990); A. J. Liu and G. S. Grest, Phys. Rev. A **44**, 7879 (1991); L. Monette, A. J. Liu, and G. S. Grest, *ibid*. **46**, 7664 (1992).

[6] W. G. Madden and E. D. Glandt, J. Stat. Phys. **51**, 537 (1988); J. A. Given and G. Stell, J. Chem. Phys. **97**, 4573 (1992); C. Vega, R. D. Kaminsky, and P. A. Monson, *ibid*. **99**, 3003 (1993); E. Lomba, J. A. Given, G. Stell, J.-J. Weis, and D. Levesque, Phys. Rev. E **48**, 233 (1993); M. L. Rosinberg, G. Tarjus, and G. Stell, J. Chem. Phys. **100**, 5172 (1994).

[7] D. M. Ford and E. D. Glandt, Phys. Rev. E **50**, 1280 (1994); R. D. Kaminsky and P. A. Monson, Chem. Eng. Sci. **49**, 2967 (1994).

[8] E. Pitard, M. L. Rosinberg, G. Stell, and G. Tarjus, Phys. Rev. Lett. **74**, 4361 (1995).

[9] A preliminary report of this work is given by K. S. Page and P. A. Monson, Phys. Rev. E **54**, R29 (1996).

[10] R. Evans, J. Phys.: Condens. Matter **2**, 8989 (1990).

[11] E. Pitard, M. L. Rosinberg, and G. Tarjus, Mol. Sim. (to be published).

[12] R. D. Kaminsky and P. A. Monson, J. Chem. Phys. **95**, 2936 (1991).

[13] W. A. Steele, *The Interaction of Gases with Solid Surfaces* (Pergamon, Oxford, 1973).

[14] J. M. D. MacElroy and K. Raghavan, J. Chem. Phys. **93**, 2068 (1990); J. M. D. MacElroy, Langmuir **9**, 2682 (1993).

[15] J. D. Weeks, D. Chandler, and H. C. Andersen, J. Chem. Phys. **54**, 5237 (1971).

[16] M. P. Allen and D. J. Tildesley, *Computer Simulation of Liquids* (Clarendon, Oxford, 1987).

[17] P. B. Balbuena and K. E. Gubbins, Langmuir **9**, 1801 (1993).

[18] J. K. Johnson, J. A. Zollweg, and K. E. Gubbins, Mol. Phys. **78**, 591 (1993).

[19] See, for example, J. R. Henderson, P. Tarazona, F. van Swol, and E. Velasco, J. Chem. Phys. **96**, 4633 (1992).

[20] J. E. Finn and P. A. Monson, Phys. Rev. A **39**, 6402 (1989); Y. Fan and P. A. Monson, J. Chem. Phys. **99**, 6897 (1993).

[21] W. D. Machin and P. D. Golding, J. Chem. Soc. Faraday Trans. **86**, 171 (1990); W. D. Machin and P. D. Golding, *ibid*. **86**, 175 (1990).

[22] P. C. Ball and R. Evans, Langmuir **5**, 714 (1989).